Determination of robotic melon harvesting efficiency: a probabilistic approach

Moshe Mann, Boaz Zion, Itzhak Shmulevich & Dror Rubinstein

Published online: 11 Sep 2015.

Submit your article to this journal ⧉

Article views: 144

View related articles ⧉

View Crossmark data ⧉

Citing articles: 2 View citing articles ⧉

Taylor & Francis
Taylor & Francis Group

Determination of robotic melon harvesting efficiency: a probabilistic approach

Moshe Mann[a]* , Boaz Zion[b], Itzhak Shmulevich[a] and Dror Rubinstein[a]

[a]*Department of Civil and Environmental Engineering, Technion, Haifa, Israel; [b]Institute of Agricultural Engineering, Agricultural Research Organization – The Volcani Center, Bet Dagan, Israel*

To automate the harvesting of melons, a mobile Cartesian robot is developed that traverses at a constant velocity over a row of precut melons whose global coordinates are known. The motion planner is programmed to have the robot harvest as many melons as possible. Numerous simulations of the robot over a field with different sets of randomly distributed melons resulted in nearly identical percentages of melons harvested. This result holds true over a wide range of robot dimensions, motor capabilities, velocities and melon distributions. Using probabilistic methods, we derive these results by modelling the robotic harvesting procedure as a stochastic process. In this simplified model, a harvest ratio is predicted analytically using Poisson and geometric distributions. Further analysis demonstrates that this model of robotic harvesting is an example of an infinite length Markov chain. Applying the mathematical tools of Markov processes to our model yields a formula for the harvest percentage that is in strong agreement with the results of the simulation. The significance of the approach is demonstrated in two of its applications: to select the most efficient actuators for maximal melon harvesting and determine the set of optimal velocities along a row of melons of varying densities.

Keywords: harvesting robot; performance prediction; probabilistic analysis; geometric distribution; Markov chain

1. Introduction

1.1 *Motivation*

Applying robots to automate harvesting tasks has potential to significantly increase the profitability of the agricultural sector (Pedersen et al. 2006; Pedersen, Fountas, and Blackmore 2008). While many prototypes of harvesting robots have been developed for various crops (see Belforte, Gay, and Aimonino 2006; Edan, Han, and Kondo 2008), many challenges inhibit them from being deployed commercially. These challenges include the unstructured environment of the field, the constantly changing field conditions, obstruction of fruit by leaves or other fruit and the fragileness of fruit handling (Edan, Han, and Kondo 2008), (Kassler 2001; Perry 2009).

New approaches have been sought in recent years to improve the performance of agricultural robots. One approach is to combine human workers and robots synergistically. For example, the collaboration of a human operator and robot applied to images acquired in melon fields increased target detection from 80% (robot only) to 94% and reduced the time required for detection by 20% (Bechar and Edan 2003). As an intermediate stage towards the final goal of fully autonomous robotic melon harvesters, we suggest another approach: separating the sensing system from the robotic harvester. Assuming the harvest targets (melons in this case) are mapped in the field prior to harvest (e.g. using an accurate GPS) and the robot gets a bank of targets in local coordinates, its speed of operation is no longer limited by the sensing method, but by its mechanical capabilities and the fruits' susceptibility.

Separating operations allow the strongest link – the robotic harvester – to operate independently from the weakest link – the sensing. This approach can be used when target locations are fixed in space and independent of each other (which is not the case, for example, in citrus trees, where after fruit is picked, its branch changes position due to the lighter load), and in particular for crops which can be modelled as two-dimensional crops (e.g. melons, watermelons, pumpkins). In addition, the economic infeasibility and low return of agricultural robots prevents their deployment. Optimising the robots' performance such that they become cost-effective is therefore particularly imperative in order to advance robots towards deployment in agriculture.

This article sets out to accomplish one aspect of that goal by analytically determining the harvest ratio, or efficiency, of a Cartesian robot for harvesting heavy fruit, particularly melons. If the efficiency of a harvesting robot can be easily

---

*Corresponding author. Email: mpm@tx.technion.ac.il

calculated for any given set of robot parameters and fruit distribution, then this would serve as a vital tool for designing cost-optimal robots and planning their motions. To accomplish this goal, the robotic harvesting process must be represented by a simplified model that yields a sufficiently accurate efficiency prediction, given the robot's dimensions, actuator capabilities, advancement speed, and distribution of melons. This prediction is derived using tools of probability and random processes.

1.2 *Literature survey*

Relatively few works address the performance and efficiency of robots from a probabilistic perspective, fewer still of agricultural robots. Of those that do, Viguria and Howard (2009, 2010) described the statistical properties of the global cost for algorithms of distributed robots. Probabilistic model checking was presented by Konur, Dixon, and Fisher (2012) and distributed stochastic modelling was presented by Lerman, Martinoli, and Aram Galstyan (2005) to analyse the behaviour of robot swarms. We seek to similarly apply probabilistic models, albeit simpler, to robotic harvesters.

For heavy fruit harvesting robots, various performance indices relating to throughput have been proposed. The theoretical field capacity, a standard measure of the rate of harvest for agricultural machines (Field and Solie 2007; Srivastava et al. 2006), was modified by Sakai, Osuka, and Umeda (2004) to measure the work capacity of watermelon harvesting robots. Edan and Miles (1993, 1994) conducted a thorough examination of how the dependence of the cycle time and harvest percentage of a melon harvesting robot are affected by the number of manipulators, actuator speeds, advancement speeds and mode of operation. However, no mathematical analysis was developed to account for that dependence. It is that analysis that we present in this article.

1.3 *Methods and materials*

The study presented here is the second part of an attempt to develop a robotic harvester for two-dimensional crops such as melons. The first part, calculating the trajectory of the robot that results in the maximum number of melons harvested, was already addressed by Mann et al. (2014b). Here, we seek to determine the expectation value of the harvest ratio given the robot and field parameters.

This is accomplished in Section 2 by first constructing a simplified model of the robotic harvesting procedure in which the manipulator picks each fruit in a uniform, cyclical motion. Then, in Section 3, probability theory is used to determine the average range of that motion. As will be shown, though, that range is larger at low robot velocities than predicted by those methods. To account for this result, the theory is extended in Section 4 by remodelling the robotic harvesting process as an infinite length Markov chain. This process is used to derive a formula predicting its ratio of successfully harvested fruit. Finally, examples of simulations are shown demonstrating the utility of this approach in Section 5. All of the simulations and analytical results in the article were carried out in MATLAB 2010b.

It is assumed throughout this article that the locations of the melons are known beforehand and are randomly distributed throughout the row with a uniform distribution. While a uniform distribution does not accurately model fruit distributions in real life, it enables the performance of the robotic harvester to be analysed probabilistically. In addition, the results can be used as an upper limit of performance of actual harvesting robots.

2. Model description

2.1 *Original model*

The robot consists of an $X–Y–Z$ Cartesian manipulator mounted on a rectangular frame that travels along a row of fruit at velocity v_t, as shown in Figure 1. The location of all melons is assumed to be known beforehand. Each picking cycle consists of a place phase – where the manipulator picks a melon off the ground and places it on one of two longitudinal conveyors, and a reach phase – where the manipulator reaches for the next melon. The time it takes the gripper to grasp the fruit, place it on a conveyor, and get back to a ready-to-pick position are assumed constant. The $x–y$ velocity and acceleration of the manipulator relative to the platform are bounded by v_{max} and a_{max}, respectively (Figure 2).

The goal of the robot is to pick up as many melons as possible by the time it reaches the end of the row. This is an example of a problem in combinatorial optimisation known as the orienteering problem with time windows. A detailed discussion of the problem and a strictly optimal algorithm to solve for it was presented by Mann et al. (2014b).

In this article, we seek to analytically predict the expected harvest ratio, or efficiency, for a range of platform velocities. Simulations were run for 120 different instances of platform velocities over rows with densities of two and three melons per square metre distributed randomly, as shown in Figure 3. Notice that the efficiency steadily decreases with increasing platform velocity. While this is to be expected because of the greater number of melons the robot must pass
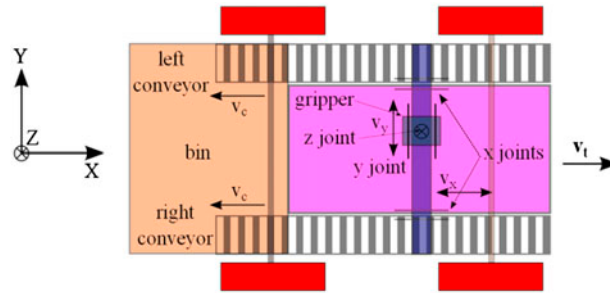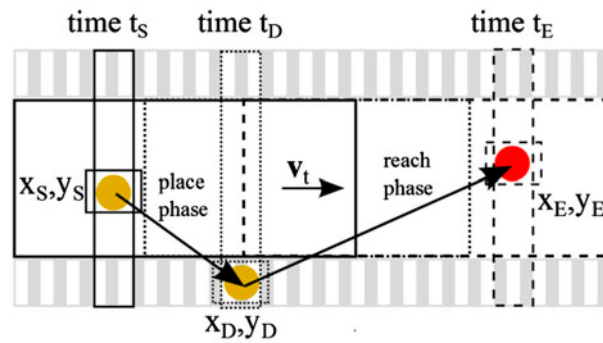
Figure 1.   Schematic of robotic melon harvester.

Figure 2.   Time lapse sequence of melon harvesting. The manipulator reaches for melon 1 at time t_S at coordinates $[x_S y_S]$, places it on the conveyor belt at time t_D at coordinates $[x_D y_D]$, and then reaches for melon 2 at time t_E at coordinates $[x_E y_E]$, repeating the cycle.
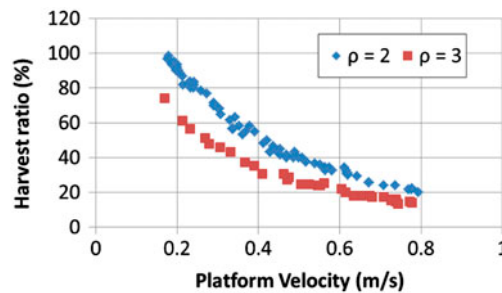

Figure 3.   Simulation results of the harvest ratio of robot for a range of platform velocities along a row of melons with an average density 2 melons/m^2 (blue) and 3 melons/m^2 (red). The ratio declines steadily with increasing velocity but is nearly constant for given robot and field parameters. Robot simulation parameters are delineated in Mann et al. (2014a).

over, what is notable is the negligible scatter, resulting in a nearly uniform harvest ratio given the platform velocity. This strongly suggests that a simpler model can accurately account for the efficiency of the robotic melon harvesting process, thus constituting the motivation for this research. It is assumed throughout the article that the melons are randomly distributed throughout the row with a uniform distribution. However, other distributions can be dealt with similarly.

2.2 *Simplified model*

To construct a simplified model that yields the simplified harvest ratio, we begin by 'folding' the melon row and robot in half, as shown in Figure 4. In this simplified model, there is only one conveyor and the density of the melons is twice as much. Each picking cycle undergoes the same uniform motion – reaching for the melon, placing it on the single conveyor, and repeating ad infinitum. By folding the workspace, the manipulator's motion is projected onto a single conveyor.
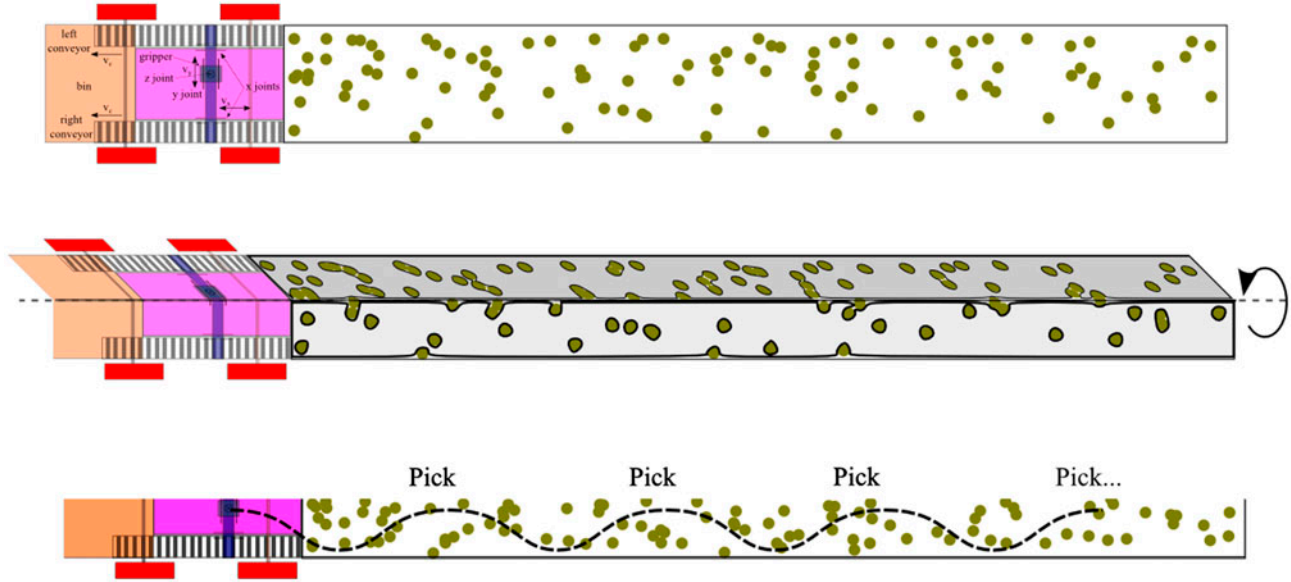
Figure 4. In the simplified model, the field and robot are folded in half. Here, there is only one conveyor, and the fruit density is double.

The logic behind the folding reflects upon the optimal path traversals selected by the combinatorial optimisation procedure. The melons lying closer to the top and bottom edges of the mobile platform require smaller traversal time between them, since they are in close lateral proximity to the conveyor belts. Therefore, the more quick traversals are selected by the robot, the more melons on average it will succeed in harvesting, as this enables the robot to pick up more fruit within the allotted time.

Thus, on average, the combinatorial optimisation algorithm will result in the manipulator spending most of its time on the fruit near the lateral edges of the platform. This means that the manipulator will make very few traversals from one conveyor to another. Folding the workspace thereby encapsulates the pattern of the manipulator's motion by representing it as occurring back-and-forth from the conveyor.

The total lateral displacement for reach and place stages combined can never exceed the width of the platform. The average lateral displacement is thus no greater than the half-width. This is accurately reflected in the simplified model, which takes advantage of the symmetry of the row to mirror the pick and place motions onto one half of the row.

This folding helps to visualise the averaged robotic motion as a uniform periodic motion. In practice, the denser the field is, the less lateral distance the manipulator must traverse on average between successive melons. In the simplified model, this translates into shorter lateral distance from melon to conveyor. This connection would not be apparent in the actual robot where the manipulator spans the entire row width. The simplified model can be easily analysed for average lateral displacement and cycle time.

The advantage of the simplified model lies in the fact that the length of the row of melons does not matter. If it is long enough, the resultant harvest ratio will converge to nearly a constant. This allows us to eliminate the row length as a parameter upon which the harvest ratio is dependent on. The main advantage, though, is that the harvest ratio of the entire process can be represented in the simplified model by the harvest ratio of a single cycle. The simplified model is thus defined by a repetitive, monotonous picking cycle.

Denoting the average displacement in the lateral y direction as y_{avg}, the time required for the manipulator to execute this motion is $T(y_{\text{avg}})$. For Cartesian manipulators with velocity and acceleration limits, $T(y_{\text{avg}})$ is an explicit formula that is provided in Table 1 in Mann et al. (2014a). For endpoint velocities of zero (when the melon is either picked or placed), the time required is simply that of a trapezoidal velocity profile, given by:

$$T(y_{\text{avg}}) = \frac{y_{\text{avg}}}{v_{\text{max}}} + \frac{v_{\text{max}}}{a_{\text{max}}} \tag{1}$$

where v_{max} and a_{max} are the respective maximum velocity and acceleration limits.

Table 1. Maximum accelerations in the *x* and *y* directions for three different harvesting robots.

	max. *x* acc. (m/s^2)	max. *y* acc. (m/s^2)
Robot 1	1	8
Robot 2	2	5
Robot 3	3	3

The harvest ratio of a cycle is the number of melons picked per cycle (which is one) divided by the number of melons passed over by the robot in this time, $2T(y_{\mathrm{avg}})\rho v_t W$. The average harvest ratio per cycle η of the simplified model is thus given by:

$$\eta = \frac{1}{2T(y_{\mathrm{avg}})\rho v_t W} \tag{2}$$

where v_t is the robot forward velocity, ρ is the melons' density, and W is the width of the row. As noted, the efficiency of the simplified model is independent of the length of the row L, and so, L does not appear in Equation (2). A comparison of the simulated harvest ratio of a 2-m long robot with the ratio given by Equation (2) and detailed in Mann et al. (2014a) is shown in Figure 5 for a robot picking up melons from rows of increasing lengths. Clearly, as the length of the row increases, Equation (2) becomes a better approximation of the efficiency due to the increasing number of cycles that are averaged out. This verifies the accuracy of the simplified model.

The advantage of the simplified model is now obvious. In this model, the efficiency of the robotic harvest depends on only one variable – y_{avg} – the average lateral manipulator displacement. It now remains to determine that displacement, and to this end, we make use of some probability distributions.

3. Probabilistic analysis

For a Cartesian manipulator, the time $T(x, y)$ required to reach any point (x, y) is given by the l_∞ norm:

$$T(x,y) = \max(T_x, T_y) \tag{3}$$

where T_x and T_y are the respective times required for manipulator to traverse x and y independently. For a manipulator with given velocity and acceleration limits, contours of points with equal reach times are thus shown in Figure 6. The time rings L_T are defined as very thin areas containing all points with reach times infinitesimally close to T:

$$L_T = \left\{ x, y : \left| \max(T_x, T_y) - T \right| \le \delta, \quad \delta \to 0 \right\} \tag{4}$$

We vary the thickness of each ring so that it is of equal area; therefore, the further outlying the ring is, the thinner it will be. For calculation of the traversal times, we ignore platform speed, or assume it to be zero, as explained below. For maximum harvest, the manipulator in the simplified model must reach for the nearest ring containing a melon and
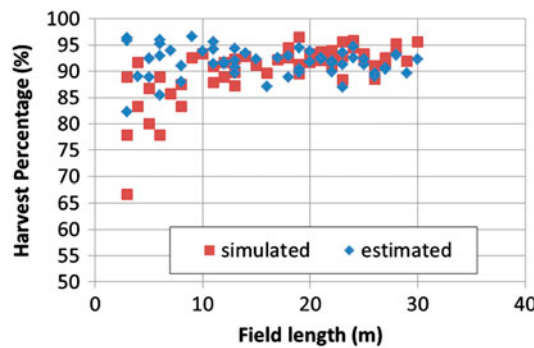

Figure 5. Robot harvest percentage for field of with 2 melons/m^2 and platform velocity 20 cm/s The analytically estimated harvest efficiency of the simplified model (blue diamonds) converges to the simulated harvest efficiency (red) as the row gets longer.
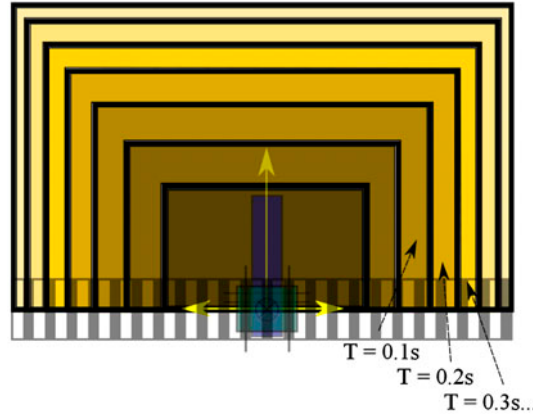
Figure 6. Rings L_T of points with nearly equal traversal times T.

then place it on the conveyor. The maximum robotic harvest problem thus becomes simplified to the finding the average nearest neighbour with respect to the conveyor.

To find it, we first assume that the melons are randomly distributed uniformly within the row. With an average density ρ, the probability of there being k melons within an area Δ is given by the Poisson probability density function:

$$f(k, \rho\Delta) = \frac{e^{-\rho\Delta}(\rho\Delta)^k}{k!}, \quad k = 0, 1, 2, \ldots \tag{5}$$

The probability of there being at least one melon within Δ is then clearly $1 - f(0, \rho\Delta)$, or $1 - e^{-\rho\Delta}$.

The average time needed to reach the nearest melon can now be given by the following theorem:

Theorem 1: *The average ring $L_{T\text{avg}}$ containing the nearest melon is that which encloses an average of one melon:*

$$L_{T\text{avg}} = \left\{ L_T : \rho \iint_{T(x,y) \leq T} \mathrm{d}x\mathrm{d}y = 1 \right\} \tag{6}$$

Proof: The chance of finding at least one melon within a ring of area Δ is $1 - e^{-\rho\Delta}$. As $\Delta \to 0$, $1 - e^{-\rho\Delta} \to \rho\Delta$. The chance of success p of any ring with infinitesimal thickness is therefore $\rho\Delta$. For trials of success rate p, the likelihood of requiring k trials to achieve the first successful trial is given by the geometric distribution $p(1 - p)^{k-1}$. The mean of the geometric distribution is $1/p$. In our case, that means that on the average, the manipulator will have to pass $1/(\rho\Delta)$ rings before finding the ring with the closest melon. The area contained in this number of rings is $\Delta \times 1/(\rho\Delta) = 1/\rho$, which also happens to be the mean area containing one melon.

□

This significant theorem yields y_{avg} – it is the distance to the ring enclosing one melon, or an area of $1/\rho$ (which would be $1/2\rho$ for the simplified model). For manipulators with equal capabilities, $T_x = T_y$, and thus $2y_{\text{avg}}^2 = 1/(2\rho)$, or

$$y_{\text{avg}} = \frac{1}{2\sqrt{\rho}} \tag{7}$$

(The multiplier '2' in $2y_{\text{avg}}^2$ results from the fact that the lateral motion of the manipulator in the equivalent model can only go upwards, while its longitudinal motion can advance left or right, as shown in Figure 6.) Plugging Equation (7) into Equations (1) and (2) yields an explicit formula for the robotic harvest ratio:

$$\eta = \frac{v_{\max} a_{\max}}{\left(a_{\max}\sqrt{\rho} + 2\rho v_{\max}^2\right) v_t W} \tag{8}$$

A comparison of Equation (7) with the actual y_{avg} of the simulated robotic harvest of a melon row 1.5 m wide is shown in Figure 7 for robot advancing at a range of platform speeds, along with the harvest ratio.

It is now clear why platform speed is irrelevant to the calculation of y_{avg}. Notice from Figure 6 that despite the declining harvest ratio for increasing speeds, the average displacement in the y direction remains relatively unchanged, in essence an invariant. This is apparently due to a 'conservation of mass' of sorts. Because the robot is advancing at a
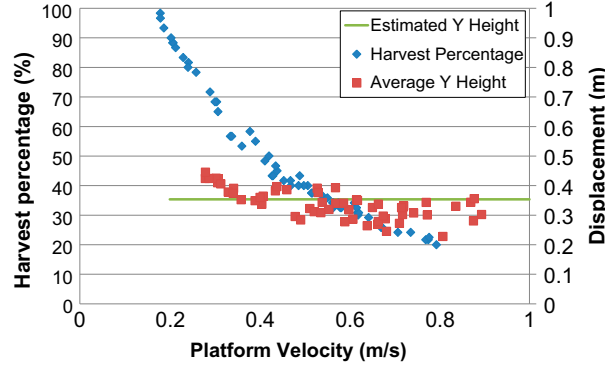
Figure 7. Harvest percentage (left axis) and average lateral displacement of manipulator (right axis) along a range of platform speeds. The estimated lateral (y direction) height derived from Equation (7) is noted by the orange line. Notice that despite the declining harvest ratio for increasing speeds, the average displacement in the y direction remains relatively unchanged.

constant speed, the rate of melons that arrive within the platform area is equal to the rate of melons that depart from it. Therefore, the manipulator does not need to stretch any farther or closer at different speeds to reach the nearest melon on average.

This method demonstrates the usefulness of the simplified model. By folding the workspace in half, the lateral displacement was decoupled from the harvest cycle time. The former depends only on the melon density, while the latter is fully deterministic given actuator limits, platform velocity and row width. The average lateral displacement is equal to the height of an envelope enclosing an average of one melon. This is an intuitive, yet non-trivial result.

4. Model extension – random processes for overlapping robot picking zones

4.1 *Random variables*

The invariance of y_{avg}, however, does not hold at low velocities. This can be seen from Figure 7: at platform velocities below 40 cm/s, y_{avg} increases. The reason for this increase is that at low velocities, the regions where the robot picks from at each cycle begin to overlap with each other. In other words, the manipulator completes a picking cycle before the robot advances the length of its frame. The average number of melons available for the next picking cycle thus decreases because the previous picking cycle depleted melons from the available region. The robotic manipulator must then travel further in order to reach a ring enclosing an average of one melon (the average nearest neighbour), and Equation (7) is no longer valid. So while the simplified model is still valid per Equation (2), a new method must be devised to determine y_{avg} for low robot velocities, i.e. at velocities the picking zones intersect.

To construct this method, we retain the simplified model while modelling the robotic harvest as a discrete time, discrete value (DTDV) random process. At each sequence i, the robot picks exactly one melon from within the envelope L_T^i. This envelope encloses an average of one melon. The random variables that describe the process are the number of melons in P_i – the region of L_T^i that does not intersect with L_T^{i+1}, and the number of melons in Q_i – the region that does intersect with L_T^{i+1} (Figure 8). We denote the former as X_{Pi} and the latter as X_{Qi}. The picked melon will be from either P_i or Q_i. The random state variable $X(i)$ is thus the Cartesian product $\{X_{Pi} \times X_{Qi}\}$.

But in order to keep the number of states finite, i.e. possible melons within L_T, we must make a minor adjustment to the probability distribution, as the Poisson distribution allows for a nonzero probability of infinite possibilities of melon quantities within L_T. We therefore assume the following regarding the melon distribution:

The number of melons within Δ is never more than $|c\rho\Delta|$, where $c > 1$ and $|c\rho\Delta|$ is the nearest integer value of $|c\rho\Delta|$.

As a rule of thumb, setting c to some value between 5 and 10 is a fairly reasonable approximation of a uniform distribution of melons in the field. From numerous trial runs, values smaller than 5 tend to distort the distribution from uniformity, and numbers larger than 10 cause a lot of computing resources to be expended in the ensuing calculations with negligible gain in accuracy. The probability distribution of melons within Δ must then be normalised. It is given by the *modified Poisson distribution* $f_{mod}(n, \rho\Delta)$:

$$f_{mod}(n, \rho\Delta) = \begin{array}{ll} \dfrac{f(n, \rho\Delta)}{cdf(n, \|c\rho\Delta\|)} & n = 0, 1, 2, \ldots, \|c\rho\Delta\| \\ 0 & n > |c\rho\Delta\| \end{array} \tag{9}$$
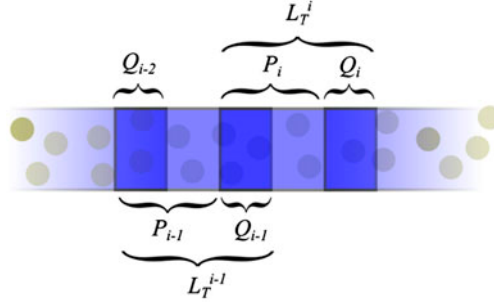
Figure 8. The pickings zones L_T^i at each discrete picking cycle i consist of the non-intersecting region P_i and the intersecting region Q_i with the following cycle. The number of melons in each region is expressed by the respective random variables X_{Pi} and X_{Qi}.

where $f(k, \rho\Delta)$ and $cdf(k, |c\rho\Delta|)$ are the respective Poisson probability density function (given in Equation (5)) and Poisson cumulative distribution function. Denoting Δ_P and Δ_Q as the respective areas of P_i and Q_i, there are thus $(|c\rho\Delta_P| + 1)\cdot(|c\rho\Delta_Q| + 1)$ possible states at i which are enumerated as $\{x_P \times x_Q\}_1, \{x_P \times x_Q\}_2, \dots$ $\{x_P \times x_Q\}_{|c\rho\Delta_P+1||c\rho\Delta_Q+1|}$ using the index k, where $k = 1, 2, \dots (|c\rho\Delta_P| + 1)\cdot(|c\rho\Delta_Q| + 1)$.

4.2 Probabilistic model

The dependence between the melon quantities at each stage i is now ready to be expressed. We model the probability that the location of the melon picked at $i - 1$ is from L_T^i as follows:

The probability $P(A_i|\{X_{Pi-1} \times X_{Qi-1}\})$ that a melon picked at $i - 1$ will intersect with LTi given the numbers of melons in each region $\{X_{Pi-1} \times X_{Qi-1}\}$ is equal to the fraction of melons in $LTi - 1$ that are located within $Qi - 1$:

$$
\begin{aligned}
P\big(A_i|\{X_{P_{i-1}} \times X_{Q_{i-1}}\}\big) &= \frac{X_{Q_{i-1}}}{X_{P_{i-1}} + X_{Q_{i-1}}} \\
P\big(\bar{A}_i|\{X_{P_{i-1}} \times X_{Q_{i-1}}\}\big) &= \frac{X_{P_{i-1}}}{X_{P_{i-1}} + X_{Q_{i-1}}}
\end{aligned}
\tag{10}
$$

where A_i is the event that the melon is picked at stage $i - 1$ from Q_{i-1} (i.e. intersects with L_T^i), $\bar{A}_i = 1 - A_i$ is the event that the melon is not picked from Q_{i-1} (i.e. picked from P_{i-1} and does not intersect with L_T^i), and $P(A_i|X)$ is the conditional probability of A occurring given that X is true. This probabilistic model is quite intuitive: The higher the proportion of melons in the intersecting area is, the more likely the robot is to pick from there.

It now remains to find an expression for the total probability $P(\{X_{Pi} \times X_{Qi}\})$ as a dependence on the previous state $\{X_{Pi-1} \times X_{Qi-1}\}$. This is accomplished using several rules of probability:

(1) Since X_{Pi} and X_{Qi} are located in separate sectors, they are independent, therefore:

$$
P\big(\{X_{Pi} \times X_{Qi}\}\big) = P(X_{Pi})P\big(X_{Qi}\big) = P(X_{Pi})f_{\mathrm{mod}}(X_{Qi}, \rho\Delta_Q)
\tag{11}
$$

(2) In the event that A_i occurred, there is one less melon presently within P_i than there was before it was picked from there. The probability distribution of melons presently located within P_i is therefore equal to the original (modified) Poison distribution *with an additional melon*, while if A_i did not occur, i.e. $\bar{A}_i$ is true, it is simply $f_{\mathrm{mod}}(k, \rho\Delta)$ from Equation (9):

$$
\begin{aligned}
P(X_{Pi}|A) &= f_{\mathrm{mod}}(X_{Pi} + 1, \rho\Delta_P) \\
P(X_{Pi}|\bar{A}) &= f_{\mathrm{mod}}(X_{Pi}, \rho\Delta_P)
\end{aligned}
\tag{12}
$$

(3) The total probability of X_{Pi} is the sum of the product of the conditional probabilities and the probability of the event upon which the condition holds true if the events are mutually exclusive. This is clearly the case here,

since the events A and $\bar{A}$ are mutually exclusive as are all possible X_{Pi-1}. Therefore, the total likelihood of X_{Pi} is given by:

$$P(X_{Pi}) = P(X_{Pi}|A_i)P(A_i) + P(X_{Pi}|\bar{A}_i)P(\bar{A}_i) \tag{13}$$

and the total likelihoods of A and $\bar{A}$ are given by, respectively:

$$P(A_i) = \sum_{\forall X_{P_{i-1}}, X_{Q_{i-1}}} P\big(A_i|\{X_{P_{i-1}} \times X_{Q_{i-1}}\}\big)P\big(\{X_{P_{i-1}} \times X_{Q_{i-1}}\}\big)$$
$$P(\bar{A}_i) = \sum_{\forall X_{P_{i-1}}, X_{Q_{i-1}}} P\big(\bar{A}_i|\{X_{P_{i-1}} \times X_{Q_{i-1}}\}\big)P\big(\{X_{P_{i-1}} \times X_{Q_{i-1}}\}\big) \tag{14}$$

Plugging Equations (10), (12) and (14) into Equation (13) and the result into Equation (11) yields the likelihood of any state $\{X_{Pi} \times X_{Qi}\}$:

$$P\big(\{X_{Pi} \times X_{Qi}\}\big) = f_{\text{mod}}(X_{Qi}, \rho\Delta_Q)$$
$$\times \sum_{\forall X_{P_{i-1}}, X_{Q_{i-1}}} \bigg(\frac{X_{P_{i-1}}}{X_{P_{i-1}} + X_{Q_{i-1}}} f_{\text{mod}}(X_{Pi}, \rho\Delta_P) + \frac{X_{Q_{i-1}}}{X_{P_{i-1}} + X_{Q_{i-1}}} f_{\text{mod}}(X_{Pi} + 1, \rho\Delta_P)\bigg) P\big(\{X_{P_{i-1}} \times X_{Q_{i-1}}\}\big) \tag{15}$$

4.3 *Markov chain*

What Equation (15) signifies is that the current state probability $P(X(i))$ depends only in the previous state's probability $P(X(i-1))$. This type of random process is known as a Markov chain. Writing the probability of each enumerated state as

$$p_k(i) = P\Big(\{X_{Pi} \times X_{Qi}\} = \{x_P \times x_Q\}_k\Big), \tag{16}$$

The vector of all possible state probabilities is denoted by:

$$\mathbf{p}(i) = \begin{bmatrix} p_1(i) & p_2(i) & \cdots p_{|c\rho\Delta_P+1||c\rho\Delta_Q+1|}(i) \end{bmatrix} \tag{17}$$

The conditional probability expressed in Equation (15) can be written in matrix form as:

$$\mathbf{p}(i)^T = \mathbf{p}(i-1)^T[A] \tag{18}$$

where $[A]$ is the $(|c\rho\Delta_P| + 1)\cdot(|c\rho\Delta_Q| + 1) \times (|c\rho\Delta_P| + 1)\cdot(|c\rho\Delta_Q| + 1)$ transition matrix of the Markov chain. The (k, l)th element of $[A]$ is defined as:

$$A(k, l) = P(\{X_{Pi} \times X_{Qi}\} = \{x_P \times x_Q\}_l|\{X_{Pi-1} \times X_{Qi-1}\} = \{x_P \times x_Q\}_k)$$
$$= f_{\text{mod}}(x_Q^l, \rho\Delta_Q)\bigg(\frac{x_P^k}{x_P^k + x_Q^k} f_{\text{mod}}(x_{P_i}^l, \rho\Delta_P) + \frac{x_Q^k}{x_P^k + x_Q^k} f_{\text{mod}}(x_P^l + 1, \rho\Delta_P)\bigg) \tag{19}$$

where x_P^k and x_{Qi}^k are, respectively, the ordinate and abscissa of $\{X_P \times X_Q\}_k$. The probability distribution at time i, using Equation (18), can then be expressed as:

$$\mathbf{p}(i)^T = \mathbf{p}(0)^T[A]^i \tag{20}$$

where $p(0)$ is the initial state vector of probabilities.

Going back to the original problem, we are looking to find the picking cycle area Δ containing an expectation value of one melon. Because the row of melons is quite long, there will be many picking cycles, and so the robotic harvest can be modelled as an infinite length Markov chain. In this case, the probability distribution for large i converges to (Ibe 2009):

$$\mathbf{p}(\mathbf{i})|_{i \to \infty} = \pi(A^T) \tag{21}$$

where $\pi(A^T)$ is the left eigenvector of A corresponding to the eigenvalue of 1. The expected value of melons within L_T^i as $i \to \infty$, $\overline{X_{Pi} + X_{Qi}}$ is then simply

$$\overline{X_P + X_Q} = \sum_{k=1}^{\left|c\rho\Delta_P+1\right|\left|c\rho\Delta_Q+1\right|} \pi_k \cdot \left(X_P^k + X_Q^k\right) \tag{22}$$

We now have a nearly analytical formula for determining the harvest ratio of the robot:

Determine the height of the average picking zone using Equation (7). If the average picking zones do not intersect, then the efficiency is given by Equation (2). If they do, then find the value of Δ (which in turn provides the value of Δ_P and Δ_Q) that causes the expected value in Equation (22) to equal 1. This can be easily executed with a nonlinear equation root finder. Obtain y_{avg}, the height of the resulting picking zone L_{Tavg}, and insert it into Equation (2), thereby providing the percentage of melons successfully harvested by the robot.

A comparison of the probabilistic method with the simulated robotic harvest ratio is shown in Figure 9 for a robot traversing a row of melons 1½ metres wide with average densities of 2 melons/m^2 (blue dots) and 3 melons/m^2 (red dots). Note that this is the same graph as in Figure 3 with the addition of the probabilistic method's result. Using the root-mean-square error (RMSE) as a goodness-of-fit test, the former yields an RMSE of .0363, and the latter of .0249. These low values indicate that the method correlates quite well with the actual values, verifying the integrity of the probabilistic approach. The y_{avg} values obtained for the respective simulations are compared with the analytical formulas in Figure 10. Here too, there is a good agreement of the simulations with the formula.

Notice in Figure 10 that y_{avg} is constant for platform velocities above the critical velocity where the average picking zones border each other, while it increases as the platform velocity decreases below the critical velocity. This is because below the critical velocity, the picking cycles zones overlap as explained in Section 4.1, while above the critical velocity, they do not overlap, and y_{avg} is accurately determined by Equation (7). Two important examples are shown demonstrating the usefulness of this method.
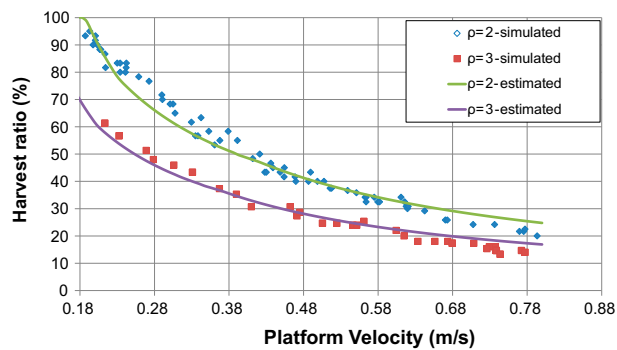

Figure 9. Harvest ratio of the robotic melon harvester as a function of the platform velocity. Simulated values are denoted by the dots, while the values obtained from the probabilistic method are represented by the solid lines.
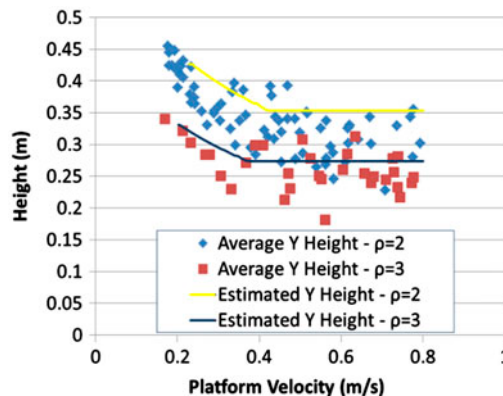

Figure 10. Corresponding values of the average lateral manipulator traversal distance as function of platform velocities. Below the critical velocity, the picking zones overlap and the manipulator must reach further to obtain the nearest melon on average.

5. Examples

5.1 *Selecting the most efficient robot*

In this example, we are to choose among three robotic harvesters with different actuator capabilities shown in Table 1 that has the highest harvest percentage. Each progressive robot number in the table has higher capabilities in the longitudinal direction but lower capabilities in the lateral direction. This means that no one robot is completely better than any other one. The robot is to harvest as many melons as possible along a row 1.5 m wide with an average density of 3 melons/m^2.

The harvest percentage of the three robots at a range of platform velocities for a row of melons computed by the models described above is shown in Figure 11. At high and low velocities, all robots perform equally the same, while at velocities of 30–40 cm/s, Robot #2 is clearly the most efficient. This demonstrates that the most efficient harvesting robot depends on its speed of advancement.

5.2 *Determining maximum platform velocity for 80% efficiency*

The objective in this example is for the robot to advance is fast as possible along the row while still being at least 80% successful. The row of melons is 36 m long, with the average density of the melons varying along the row as shown in Figure 12. We want to determine how fast the robot can advance in each sector.

The velocities and the resultant harvest percentages computed by the models above are shown in Table 2. In each sector, the robot harvest roughly 80% of the melons, and the percentage for the entire field was exactly 80.9%, which is quite close to the 80% efficiency objective. This verifies the probabilistic approach as an accurate predictor of harvesting robot efficiency.
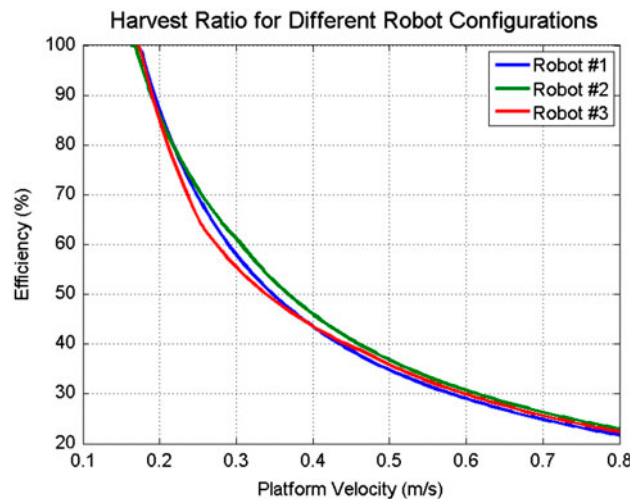

Figure 11. Harvest ratio for the three robots for range of platform velocities in Table 1.
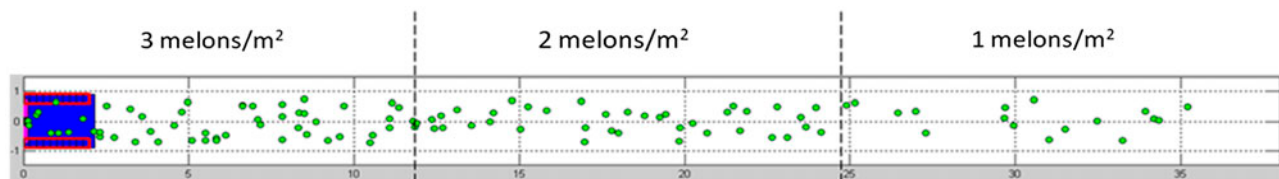

Figure 12. Robot traversing field with range of different average melon densities.

Table 2. Platform velocities required to harvest 80% of the melons along a row with section of varying mean densities.

Density (melons/m^2)	3	2	1	Total
Platform velocity (cm/s)	17	22	40	
Number of melons	54	36	18	110
Number harvested	44	31	14	89
Harvest percentage	81.5%	86.1%	77.8%	80.9%

6. Summary and conclusions

We have presented a probabilistic approach that accurately predicts the robotic harvest percentage of melons given its dimensions, actuator limits, forward velocity and melon distribution. It is based on constructing a simplified model of the robotic harvesting process in which the robot picks up each melon in a uniform, cyclical motion. That way, the harvest ratio of the entire process is equal to the harvest ratio of single cycle. The maximum robotic harvest problem then becomes simplified to the average nearest neighbour. Modelling the robotic harvest as a series of uniform manipulator cycles allows the harvest efficiency to be calculated analytically.

The nearest neighbouring melon was proven to lie on an envelope enclosing an average of one melon. This yields an analytical formula for the robotic harvesting percentage. While this formula holds for sufficiently high robot velocities, it must be modified for low robot velocities (which are most realistic for high harvest percentages) where the envelopes of each picking cycle overlap with each other. In that case, the expected value of melons within the envelope is decreased and the envelope must be enlarged to contain one melon within it. The dimensions of this envelope can be determined by modelling the robotic harvesting process as a random process represented by an infinite length Markov chain for low robot velocities.

Various principles of probability are applied to this model to yield an analytical formula for the harvest percentage. This formula has been shown to provide yield robotic harvest ratios that are in excellent agreement with simulations and is utilised for both optimal robot selection and velocity planning. While high robot velocities yield a very low harvest ratio and are unsuitable for single manipulator robots, they may be practical for multi-manipulator robots where the combined yield from each robot arm results in a highly efficient harvest.

The results derived in this article are limited to hypothetical situations where the model assumptions hold. These include the constant advancement velocity of the mobile platform, the known location of the fruits beforehand, and the lack of disturbances or uncertainties of the robot parameters. The most limiting assumption is the uniform distribution of the fruit. In reality, melons are better represented by a gamma distribution (Edan and Simon 1997). However, the results obtained can still be useful as an upper limit of performance or for robotic retrieval of objects more suited to a uniform distribution. Future research can be directed at testing and verifying the probabilistic approach on real-world robotic harvesting missions.

Disclosure statement

No potential conflict of interest was reported by the authors.

ORCID

Moshe Mann http://orcid.org/0000-0002-3813-1327

References

Bechar, A., Y. Edan. 2003. "Human-robot Collaboration for Improved Target Recognition of Agricultural Robots." *Industrial Robot: An International Journal* 30: 432–436.

Belforte, G., P. Gay, and D. R. Aimonino. 2006. "Robotics for Improving Quality, Safety and Productivity in Intensive Agriculture: Challenges and Opportunities." In *Industrial Robotics: Programming, Simulation and Applications*, edited by Kin-Huat Low, Chap. 35, 677–690. Mammendorf: Pro Literatur Verlag.

Edan, Y., and G. E. Miles. 1993. "Design of an Agricultural Robot for Harvesting Melons." *American Society of Agricultural Engineers* 36 (2): 593–603.

Edan, Y., and G. E. Miles. 1994. "Systems Engineering of Agricultural Robot Design." *IEEE Transactions on Systems, Man, and Cybernetics* 24 (8): 1259–1265.

Edan, Y., and J. E. Simon. 1997. "Spatial and Temporal Distribution of Ripe Muskmelon Fruit." *HortScience* 32 (7): 1178–1181.

Edan, Y., S. Han, and N. Kondo. 2008. "Automation in Agriculture." In *Handbook of Automation*, edited by Shimon Y. Nof, Chap. 63, 1095–1128. Dordrecht, Heidelberg, London, New York: Springer.

Field, H. L., and J. B. Solie. 2007. *Introduction to Agricultural Engineering Technology – A Problem Solving Approach*. New York: Springer.

Ibe, O. C. 2009. *Markov Processes for Stochastic Modeling*. Burlington, MA: Elsevier Academic Press.

Kassler, M. 2001. "Agricultural Automation in the New Millennium." *Computers and Electronics in Agriculture* 30: 237–240.

Konur, S., C. Dixon, and M. Fisher. 2012. "Analysing Robot Swarm Behaviour via Probabilistic Model Checking." *Robotics and Autonomous Systems* 60 (2): 199–213.

Lerman, K., A. Martinoli, and Aram Galstyan. 2005. "A Review of Probabilistic Macroscopic Models for Swarm Robotic Systems." In *Swarm Robotics Workshop: State-of-the-art Survey*, edited by E. Sahin and W. Spears, 143–152. Berlin: Springer-Verlag.

Mann, M. P., D. Rubinstein, I. Shmulevich, and B. Zion. 2014a. "Minimum Time Kinematic Motions for a Cartesian Mobile Manipulator of a Melon Harvesting Robot." *ASME Journal of Systems, Dynamics, and Control* 136 (5): 1–9.

Mann, M. P., D. Rubinstein, I. Shmulevich, and B. Zion. 2014b. "Motion Planning of a Mobile Cartesian Manipulator for Optimal Harvesting of 2-d Crops." *Transactions of the ASABE* 57: 283–295.

Pedersen, S. M., S. Fountas, H. Have, and B. S. Blackmore. 2006. "Agricultural Robots – System Analysis and Economic Feasibility." *Precision Agriculture* 7: 295–308.

Pedersen, S. M., S. Fountas, and S. Blackmore. 2008. "Agricultural Robots – Applications and Economic Perspectives." In *Service Robot Applications*, edited by Y. Takahashi, Chap. 21, 369–382. Rijeka, Croatia: InTech Education and Publishing.

Perry, T. S. January 2009. "Fruitless." *IEEE Spectrum* 46 (1): 55–58.

Sakai, S., K. Osuka, and M. Umeda. 2004. "Global Performance of Agricultural Robots." *Proceedings of the 2004 IEEE/RSJ International Conference on Intelligent Robots and Systems*. Sendai, Japan. 461–466.

Srivastava, A. K., C. E. Goering, R. P. Rohrbach, and D. R. Buckmaster. 2006. *Engineering Principles of Agricultural Machines*. 2nd ed. St. Joseph, Michigan: ASABE.

Viguria, A., and A. M. Howard. 2009. "A Probabilistic Model for the Performance Analysis of a Distributed Task Allocation Algorithm." *Proceedings of the IEEE International Conference on Robotics and Automation*. Kobe, Japan.

Viguria, A., and A. M. Howard. 2010. "Probabilistic Analysis of Market-based Algorithms for Initial Robotic Formations." *International Journal of Robotics Research* 29 (9): 1154–1172.